Numerical Modelling of Non-premixed Turbulent Combustion

Fethi BOURAS [1*], Azeddine SOUDANI [1] & Mohamed SI-AMEUR [2]

[1] LPEA, Laboratoire de Physique Energétique Appliquée, Batna University, Faculty of Science, Department of physics, 05000 Batna, Algeria.
[2] LESEI, Laboratoire des Etudes des Systèmes Energétiques Industrielles, Batna University, Faculty of Engineering, Department of Mechanical Engineering, 05000 Batna, Algeria.
[*] Corresponding Author: E-Mail: f.bouras@hotmail.fr

***Abstract*- Non-premixed turbulent flames control many practical applications of combustion. Studying these mechanisms has been the objective of numerous theoretical and experimental works, numerical simulation is also widely used to understand these flames. A brief review of numerical models for non-premixed turbulent combustion is given. This research work focuses on the coupling of Beta-PDF approach with LES model.**

In this study, we deal with the flame evolution inside the combustion chamber, this would help in protecting the walls from being overheated and might damage. On the other hand, this work focuses on, CO production and conversion in the flame zone.

The combustion system is modelled using Beta-PDF coupled with LES to predict the velocity field, CO mass fraction, and the temperature field. Our predictions are validated using the available experimental data.

The new developed model succeeded in simulating the swirling and the flame zone. The results show a good agreement with the experiment.

Key words *Non-premixed turbulent combustion, Large eddy simulation (LES), Probability density function (PDF)*

NOMENCLATURE

e	Internal energy of species	$J.Kg^{-1}$
hi	Enthalpy of species	$J.Kg^{-1}$
k	Thermal conductivity	W/m.K
M_i	Molecular mass of species i	$Kg.mole^{-1}$
p	Pressure	Pa
P(…)	Probability density function	
r	Radial coordinate	m
t	Time	s
T	Temperature	K
u_α	Velocity component	$m.s^{-1}$
x	Spatial coordinate	m
y_i	Mass fraction of species i	
Z	Mixture fraction	

Greek Symbols

δ_{ij}	Kronecker delta	
μ_t	Turbulent viscosity	$kg.m^{-1}. s^{-1}$
σ^2	Distribution variance	
ν	Kinematics viscosity	$m^{-1}. s^{-1}$
ρ	Mass density	kg/m^3
τ	Viscous stress tensor	

Notations

PDF	Probability Density Function
LES	Large Eddy simulation

I. INTRODUCTION

Turbulent combustion is among the most challenging and important subjects in theoretical and engineering sciences. It involves a range of complex physical and chemical phenomena that interact. The major physical processes include turbulent transport, chemical reaction. The difficulties of understanding turbulent combustion are further compounded by three-dimensional flows in complex geometries, such as the combustion chamber of an automotive engine.

The fundamental advantage of LES has been called into question for reacting flows. It has been argued that since chemical reactions take place only after the reactants become mixed at the molecular level (so that reactions occur mostly in the subgrid scales). One could also argue that it is because of the inaccurate modelling of the large scales, in particular large-scale mixing; LES may be able to outperform Reynolds-averaged computations that employ more sophisticated chemistry models. In many ways, LES represents a logical compromise by providing accurate, high fidelity solutions at affordable cost. Current simulation codes for single-phase turbulent combustion may be computational fluid dynamics based, with a probability density function (PDF) based approach for turbulence/chemistry interactions.

II. GOVERNING EQUATIONS

The equations governing gaseous combustion are summarized below [1], [2]. They are valid for a mixture of ideal gases in local thermodynamic equilibrium:

Mass:

$$\frac{\partial \rho}{\partial t} + \frac{\partial}{\partial x_\alpha}(\rho u_\alpha) = 0 \quad (1)$$

Momentum:

$$\frac{\partial \rho u_\beta}{\partial t} + \frac{\partial}{\partial x_\alpha}(\rho u_\alpha u_\beta) = -\nabla p + \nabla \tau + \rho \sum_i y_i f_i \quad (2)$$

Energy:

$$\frac{\partial (\rho e)}{\partial t} + \frac{\partial}{\partial x_\alpha}(\rho u_\alpha e) = -\nabla (pu) + \nabla (\tau . u) + \sum \rho V_i y_i h_i - k \nabla T \quad (3)$$

Species:

$$\frac{\partial \rho y_i}{\partial t} + \frac{\partial}{\partial x_\alpha}(\rho u_\alpha y_i) = -\nabla (\rho V_i y_i) + \rho w_i \quad (4)$$

Where: $\alpha = 1,2,3$ and $\beta = 1,2,3$

Thermodynamic State:

$$p = \rho \sum_i \frac{y_i}{M_i} RT \quad (5)$$

Quantities per unit volume are treated using a Reynolds decomposition [1,3 &4],

$$\rho = \overline{\rho} + \rho' \quad (6)$$

While quantities per unit mass are best described by a Favre (density-weighted) decomposition [1,3 &4]

$$u = \widetilde{u} + u'' \quad (7)$$

Where:

$$\widetilde{u} = \overline{\rho u} / \overline{\rho} \quad (8)$$

The majority of the models of subgrid are based on the assumption of Boussinesq which present the tensor of the unsolved constraints τ_{ij} to the tensor velocity of deformation $\widetilde{S}_{ij}$ by the intermediary of a turbulent viscosity,

The small scales influence the large scales via the subgrid-scale stress [3],[4]:

$$\tau_{ij} = 2\mu_T \left(\widetilde{S}_{ij} - \frac{1}{3} \widetilde{S}_{ll} \delta_{ij} \right) \quad (9)$$

The filtered strain rate tensor is defined by

$$\widetilde{S}_{ij} = \frac{1}{2} \left(\frac{\partial \widetilde{u}_i}{\partial x_j} + \frac{\partial \widetilde{u}_j}{\partial x_i} \right) \quad (10)$$

The residual stress tensor of the Smagorinsky eddy viscosity model can be found as [5],[6]&[7]:

$$\mu_T = \overline{\rho} C_s \Delta_x^2 \left| \widetilde{S}_{ij} \right| = \overline{\rho} C_s \Delta^2 \sqrt{\widetilde{S}_{ij} \widetilde{S}_{ij}} \quad (11)$$

C_s Smagorinsky model constant (*Cs=0.18*), and Δ is the spatial filter width which is generally related to the grid size of the resolved field.

III. BETA-PDF

Very little work in applying mapping closure for turbulent reacting scalars has been done since its original conception by Chen *et al.* (1989) and generalization for multiple reactive scalars by Pope (1991). Jiménez *et al.* (1997) demonstrated the good performance of the beta- PDF model using data from a highly intermittent, incompressible, turbulent mixing layer. It has also been shown (Wall *et al*. 2000; Cook and Riley 1994) that accurate prediction of the subgrid variance is the most important factor in obtaining good results with the beta PDF [1], [6].

When Favre filtering is used for the scalar variables, it is more appropriate to evaluate filtered quantities using the joint Favre PDF of the subgrid scalar fluctuations. Analogous to the state relation for density (5), Favre-filtered quantities would be evaluated using [1],[8],

$$\widetilde{y} = \int y(\phi_1, \phi_2, ...) \widetilde{P}(\phi_1, \phi_2, ...) d\phi_1 \, d\phi_2 ... \quad (12)$$

In the assumed PDF method, the probability density function is modeled directly using simple analytical forms, such as the beta distribution. However, because source terms can directly modify the PDF of a scalar, the beta distribution can be expected to be valid only for conserved scalars. For this reason, it is applied only to mixture fraction in this work.

In Beta distributions the probability density function on the interval, $0 \le x \le 1$, is given by[1,7],

$$P(x;\alpha,\beta) = x^{\alpha-1}(1-x)^{\beta-1}\frac{\Gamma(\alpha+\beta)}{\Gamma(\alpha)\Gamma(\beta)} \qquad (13)$$

α And β are related to the distribution mean and variance (μ,σ). Where given by [1], [8]:

$$\begin{cases} \alpha = \dfrac{\mu(\mu-\mu^2-\sigma^2)}{\sigma^2} \\ \beta = \dfrac{(1-\mu)(\mu-\mu^2-\sigma^2)}{\sigma^2} \end{cases} \qquad (14)$$

IV. EXPERIMENTAL CONFIGURATION AND THE COMPUTATIONAL DOMAIN

The experimental study used for the validation of the simulation methodology was the coaxial jet combustor configuration of Charles David pierce (2002). This experiment was chosen for its relatively simple geometry and boundary conditions yet complex flow patterns resembling those in a gas turbine combustor, and for the availability of detailed measurements that map the species, temperature, and velocity fields within the combustor.

Combustion chamber to two coaxial jets: The central jet, of inner radius R1 and outer radius R2, injects methane with a velocity V1 and a temperature T1; and the annular jet, of radius R3, injects air with a velocity V2 and a temperature T2, in a combustion chamber of radius R4 with isothermal walls.

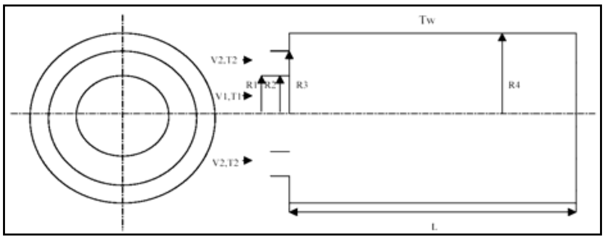

Figure 1: Schematic of the coaxial jet combustor experiment

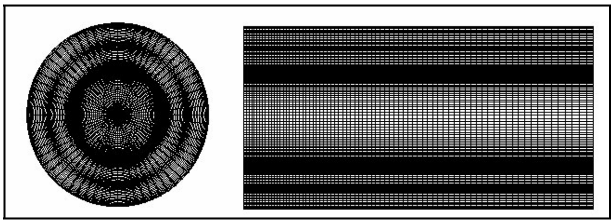

Figure 2: Schematic diagram of the computational domain and grid.

A picture of the grid used for all of the simulations is shown in Figure 2. The grid used is of the hybrid type so that prisms are selected in the centre and of the parallelepipeds in the remainder of the field of study of the combustion chamber. The distribution of grid points was not determined by any systematic rules, but rather by experience and trial-and-error, although general requirements are that the grid be smooth and be refined near solid boundaries and in particular in the axial direction at the jet orifice.

V. RESULTS

In this section, results for the Beta-PDF chemistry models are examined and compared to each other and to experimental data. The most important question to be answered is whether the simulation methodology is capable of accurately capturing the gross characteristics and behavior of the flame, such as the rate of product formation and heat release, flame lift-off, ignition, and extinction. Characteristics that depend on the details of the combustion process, such as

Large eddy simulations approach of the coaxial jet combustor illustrated in figure 1. This experiment was chosen for its relatively simple geometry and boundary conditions. The fuels used are methane and air. In this party, results for the chemistry models compared to experimental data. The obtained predictions using this approach present a good agreement with experiments.

V.1. Velocity

Axial velocity and axial fluctuation intensity results are shown in Fig.3. Where a good agreement with experimental results is achieved.

The creation of the zones of recirculation upstream close to the walls is due to the abrupt widening of the combustion chamber generating a brutal variation of the parameter (surface, pressure...), what can be explained by the significant negative values observed close to the wall (Fig.3).

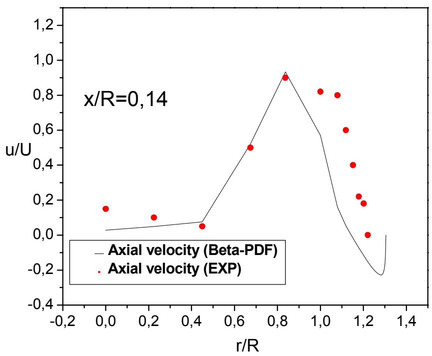

Figure 3(a): Radial profiles of axial velocity x/R=0.14

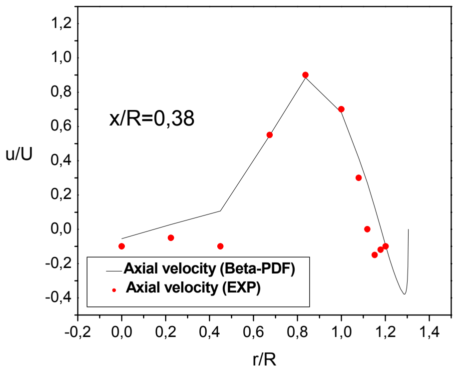

Figure. 3(b): Radial profiles of axial velocity x/R=0.38

One second zone of recirculation, caused by the delayed flow, appeared in the centre of the combustion chamber. The delayed methane flow produces shearing which give rise to this zone of recirculation. The zone of the flame is the seat of the great values velocity.

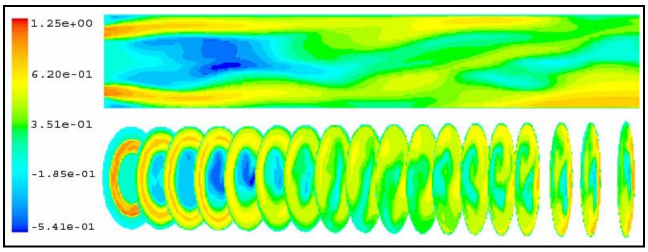

Figure 4: Instantaneous axial velocity distribution

V.2. *Temperature*

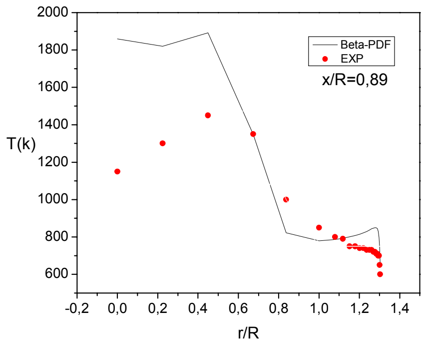

Figure 5(a): Radial profiles of temperature x/R=0.89

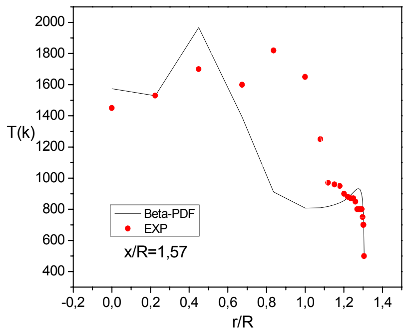

Figure 5(b): Radial profiles of temperature x/R=1.57

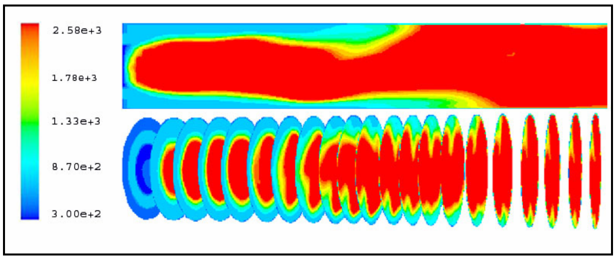

Figure 6: Instantaneous temperature distribution

In this study the wall are considered non-adiabatic (isothermal walls). Comparison of predicted temperature profiles with experimental data is shown in Fig. 5. Temperature is in good agreement with experimental data. Since the experiment had isothermal, water-cooled walls at roughly 500K, thermal boundary layers would be expected to develop, affecting the temperature close to the wall.

V.3. *Carbon monoxide "CO"*

The results clearly show that Beta-PDF approach has room for improvement in upstream of combustor.

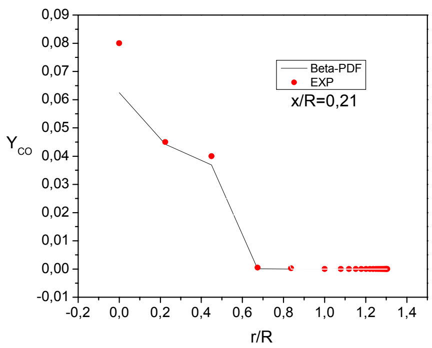

Figure 7(a): Radial profiles of CO mass fraction x/R=0.21

Fig.7 presents the *CO* results of our simulation compared with experimental data. *CO* is a significant species in the fuel-rich interior region of the flame. Because dissipation rates are low in this region, a good agreement with experimental data is observed.

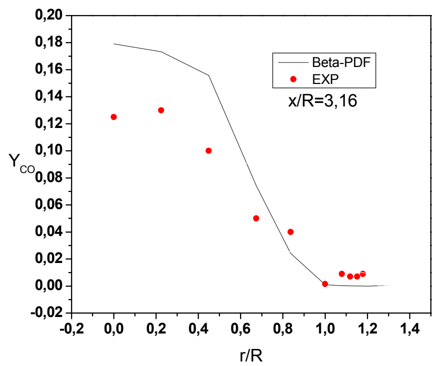

Figure 7(b): Radial profiles of CO mass fraction x/R=3.16

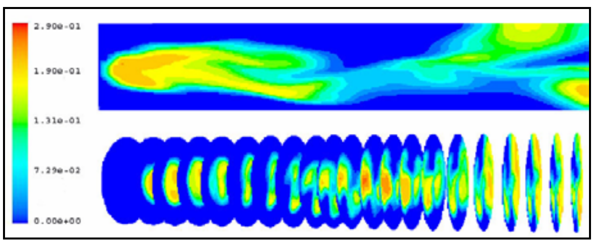

Figure 8: Instantaneous CO mass fraction distribution

The results obtained shows that the temperature behaves same manner as the fraction of mass of CO. The temperature is high in the zone of the flame and it decreases as one move away from the flame. It is the same tendency observed for the evolution of the mass fraction of CO.

VI. CONCLUSION

Large eddy simulation was shown to be a promising technique for the prediction of complex turbulent reacting flows. In the present work, we used the algorithm for large eddy simulation of variable density reacting of flows in simple combustor configurations. Particular attention was given to the conservation (mass, momentum, scalar). The results obtained of simulation in this study shows that the field of velocity is sensitive to heat, chemistry and the geometry. What can be explained by the pike in the profiles of velocity in the area of the flame on the one hand and on the other hand by the presence of the troughs of low pressure due to the geometry of the burner and the gradient velocity between the two jets. The zone of recirculation is caused in the centre of the combustion chamber in order to hang the flame. A good agreement was obtained between computations and the experiment in velocity profiles, fluctuating velocity profiles, temperature profiles, and CO mass fraction profiles.

The Beta-PDF for LES used in the present study does not account for the effects of subgrid fluctuations on scalar dissipation rate or for reaction front propagation in premixed and partially premixed combustion.

Future improvements of this model should include both the effects of dissipation rate and the chemical source term in the assumed shape of the PDF.

The most recent class of new combustion models allows the analysis of complex phenomena like the formation and the destruction of pollutants and acoustic effect in modern combustors.

REFERENCES

[1] C. David Pierce, Progress-variable approach for large-eddy simulation of turbulent combustion, PhD, Stanford university, 2001.

[2] K Tajiri and S Menon, Simulations of Combustion Dynamics in Pulse Combustor, Atlanta, Georgia 30332-0150, USA, Technical Report TR-01-010, December 2001.

[3] J. U. Schluter, X. Wuy, S. Kimz, J. J. Alonso and H. Pitsch. Coupled RANS-LES Computation of a Compressor and Combustor in a Gas Turbine Engine. 40th AIAA/ASME/SAE/ASEE Joint Propulsion Conference and Exhibit July 11-13, 2004

[4] L. Selle, Simulation aux grandes échelles des interactions flamme/acoustique dans un écoulement vrillé, Docteur, INP Toulouse, 2004.

[5] J. Schluuter, Influence of axisymmetric assumptions on large eddy simulations of a confined jet and a swirl flow, CERFACS Toulouse, 2001.

[6] S. Cheol Ko & H. Jin Sung, Large-scale turbulent vortical structures inside a sudden expansion cylinder chamber, Flow, Turbulence and Combustion, Vol.68: pp.269–287, 2002. Kluwer Academic Publishers.

[7] H. Xue, J.C. Ho, Y.M. Cheng .Comparison of different combustion models in enclosure fire simulation. Fire Safety Journal (2001) 36 :3754

[8] Y. Wu, D.C. Haworth , M.F. Modest B. Cuenot .Direct Numerical Simulation of Turbulence/Radiation Interaction in Premixed Combustion Systems. Colloquium 5: Turbulent Flames,2003.